Autonomous Underwater Vehicles Conducting Mine Counter Measure Exploratory Operations

Dr. Bao Nguyen
DRDC Atlantic/DRDC CORA

David Hopkin
DRDC Atlantic

Dr. Handson Yip
NATO Undersea Research Centre

DRDC CORA TM 2008-042
October 2008

Defence R&D Canada
Centre for Operational Research and Analysis

Central Operational Research Team

National Defence Défense nationale

Canada

Autonomous Underwater Vehicles Conducting Mine Counter Measure Exploratory Operations

BAO NGUYEN
DRDC CORA & DRDC ATLANTIC

DAVID HOPKIN
DRDC ATLANTIC

HANDSON YIP
NATO UNDERSEA RESEARCH CENTRE

Defence R&D Canada – CORA

Technical Memorandum

DRDC CORA TM 2008-042

October 2008

Principal Author

Original Signed by Bao Nguyen

Dr. Bao Nguyen

Approved by

Original Signed by Paul Massel

P. Massel

Team Leader – Central Operational Research Team

Approved for release by

Original signed by Dr. R. Mitchell

Dr. R. Mitchell

Acting Chief Scientist

The information contained herein has been derived and determined through best practice and adherence to the highest levels of ethical, scientific and engineering investigative principles. The reported results, their interpretation, and any opinions expressed therein, remain those of the authors and do not represent, or otherwise reflect, any official opinion or position of DND or the Government of Canada.

Defence R&D Canada – Centre for Operational Research and Analysis (CORA)

Abstract

Recent improvements in Autonomous Underwater Vehicle (AUV) technologies are making them increasingly attractive as mine hunting platforms by extending the reach of the sensors and weapons that are used in these operations. In this paper, we describe novel concepts of operations for AUVs performing Mine Counter Measure (MCM) exploratory operations. These concepts maximize the MCM effectiveness and minimize resources in MCM exploratory operations. In particular, the paper describes how previously un-modelled characteristics such as the aspect and range dependencies of mine detection show a significant influence on the mission effectiveness of a side scan sonar based system.

Résumé

De récentes améliorations survenues dans la technologie des véhicules sous-marins autonomes (AUV) rendent ceux-ci de plus en plus intéressants en tant que plate-formes de chasse aux mines; on a notamment amélioré la portée des capteurs et des armes utilisés dans ce genre d'opérations. Le présent document expose des concepts d'exploitation novateurs pour les AUV avec lesquels on effectue des missions exploratoires pour la lutte contre les mines (LCM); ces concepts maximisent l'efficacité de la LCM tout en réduisant à un minimum les ressources qui y sont consacrées. On y décrit, notamment, comment certaines caractéristiques non modélisées jusqu'à maintenant (comme le fait que la détection des mines est tributaire de l'angle d'aspect et de la distance) peuvent avoir une forte incidence sur l'efficacité de la mission lorsqu'on utilise un système sonar à balayage latéral.

This page intentionally left blank.

Executive summary

Mine Counter Measure (MCM) exploratory operation aims to determine the presence or absence of mines in an area of operation. It is an essential operation preceding the deployment of high-value asset when undertaken in potentially mined waters. The use of Autonomous Underwater Vehicles (AUVs) in an MCM exploratory operation is relatively recent. Hence, effective concepts of operations are lacking. In this paper, we will focus on two key measures of performance that characterize the effectiveness and efficiency of the Dorado mission plan, a Remotely Operating Vehicle (ROV) developed.

We consider the probability of detection as a function of range and the probability of detection as a function of aspect angle that are characteristics of the Dorado. Based on these assumptions, we found that to eliminate the gaps in detection range, the Dorado can employ an uneven lawn mowing search pattern as shown below. In addition, a rule of thumb was found to optimize the angular probability of detection that is derived from multiple looks at a same target. For example, an optimal two look search pattern consists of two perpendicular uneven lawn mowing search patterns as also shown below. An optimal three look observation consists of three legs that differ by $60\ \text{deg}\left(\frac{\pi}{3}\right)$. That is, the first leg makes a zero angle with respect to the horizontal axis, the second leg makes a $60\ \text{deg}$ with respect to the horizontal axis and the third leg makes a $120\ \text{deg}$ with respect to the horizontal axis. This rule of thumb provides to the operators a simple, robust and effective concept of operations.

The results for one AUV are used to model a MCM exploratory operation that involves multiple AUVs. We found the optimal search pattern as described above affect the resource allocation and the effectiveness of a MCM exploratory operation.

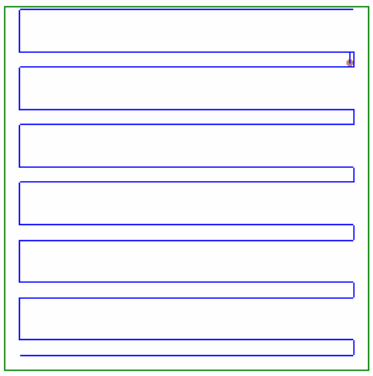

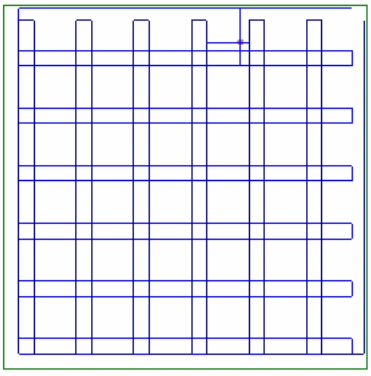

Figure 1. *Uneven lawn mowing patterns*

The number of possible missions with AUVs is growing such as MCM operations, intelligence & surveillance and reconnaissance, and barrier patrol. These missions will be interesting and relevant and will be analyzed in the future. This could include the concept of collaborative AUVs.

Nguyen, B. U., David Hopkin and Handson Yip. 2008. Autonomous Underwater Vehicles Conducting Mine Counter Measure Exploratory Operations. DRDC CORA TM 2008-042 DRDC CORA.

Sommaire

Les missions exploratoires de lutte contre les mines (LCM) visent à déterminer s'il y a ou non des mines dans une aire d'opération quelconque. Il s'agit-là d'une activité essentielle préalable au déploiement d'actifs coûteux dans des zones susceptibles d'être minées. L'utilisation de véhicules sous-marins autonomes (AUV) pour de telles missions est relativement récente. Conséquemment, on note un manque de concepts d'exploitation efficaces en cette matière. Nous nous pencherons donc, dans le présent document, sur deux mesures clé du rendement caractérisant l'efficacité et l'efficience du plan de mission du *Dorado*, le véhicule téléguidé (VTG) qui a été mis au point.

Nous considérons la probabilité de détection comme une fonction de la distance et de l'angle d'aspect caractéristiques du *Dorado*. En nous basant sur ces hypothèses, nous avons constaté que, pour éliminer les lacunes de portée en détection, le *Dorado* peut employer un circuit de recherche irrégulier du type « tonte de pelouse » conforme à l'illustration ci-dessous. On a en outre découvert une recette empirique pour optimiser la probabilité angulaire de détection; cette dernière est dérivée de visées multiples d'un même objectif. Ainsi, un circuit de recherche optimal à double visée consiste à effectuer deux parcours de recherche irréguliers et perpendiculaires du type « tonte de pelouse », tel qu'illustré ci-après. Une observation optimale à trois visées consiste en trois parcours ayant un écart angulaire de soixante degrés [$60 \deg \left(\frac{\pi}{3} \right)$]. Autrement dit, le premier parcours correspond à l'axe horizontal, le deuxième s'en écarte de 60 degrés, alors que le troisième fait un angle de 120 degrés avec l'horizontale. Cette recette empirique donne à l'opérateur un concept d'exploitation simple et robuste.

Les résultats d'un AUV sont utilisés pour modéliser une mission exploratoire faisant intervenir plusieurs appareils. Nous avons constaté que le circuit de recherche optimal décrit ci-dessus avait une incidence sur l'affectation des ressources et l'efficacité d'une mission de LCM.

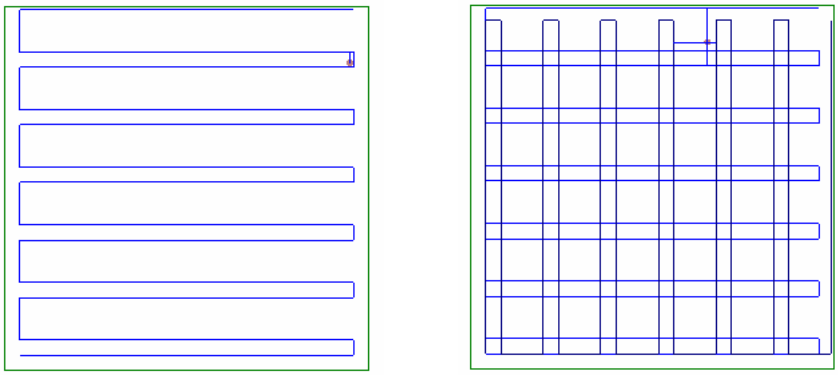

Figure 2. *Circuits de recherche irréguliers du type « tonte de pelouse »*

Les possibilités de recours aux AUV pour diverses missions, telles que les opérations de LCM, les activités de surveillance, de reconnaissance et de renseignement, ainsi que les patrouilles de barrière, se multiplient. De telles missions sont pertinentes et d'un intérêt certain. Nous ne manquerons pas d'en faire l'analyse dans l'avenir, y compris, éventuellement, l'étude du concept d'AUV collaboratifs.

Nguyen, B. U., David Hopkin and Handson Yip. 2008. Autonomous Underwater Vehicles Conducting Mine Counter Measure Exploratory Operations. DRDC CORA TM 2008-042 DRDC CORA.

Table of contents

List of figures

List of tables

Acknowledgements

The authors wish to thank the reviewers for comments that improve the quality of the report.

This page intentionally left blank.

1. Background

A frequent and important naval MCM operation is called an MCM Exploratory Operation (also known as an MCM reconnaissance operation). The aim of an MCM exploratory operation is to determine the presence or absence of mines in an area of operation. It is an essential operation required before any high-value asset is deployed in potentially mined waters. If a mine is detected, classified, and identified during exploratory operations, then mine clearance operations will follow.

The use of AUVs in an MCM exploratory operation is relatively recent. The knowledge to use them in an efficient and effective way is limited. In this paper, we will focus on two key metrics that characterize the efficiency and effectiveness of the AUV mission plan. The first metric is the confidence that there are no mines or there are mines in the search areas. The second metric is the time required to gain that confidence level.

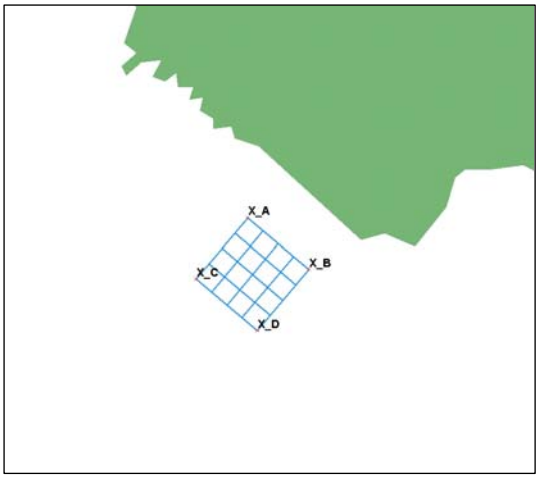

Figure 3. *Search areas*

2. Introduction

Any search strategies must take into account the current mind-set and operating practices of the operator, and the technological constraints of today's AUV systems. The preferred way of conducting an exploratory search of a large area is to segment that area such that short missions are conducted in the segmented areas. For example, an operator would plan an AUV mission such that the AUV would bring back data for analysis within a few hours. In this paper, we consider an area that has been partitioned into sixteen 3 km x 3 km square cells as shown in Fig. 2.

Table 1. *Scenario parameters*

PARAMETERS	VALUES
Total area: 16 segmented areas	12 km by 12 km
Segmented area	3 km by 3 km
AUV Speed	9 knots
Endurance	30 hours

2.1 Assumptions

In this paper, we assume the AUV carries a side scan sonar. The mine hunting environment plays an important role in the performance of the side scan sonar or any MCM sensor for that matter. Seabed conditions, such as clutter, composition and topology have the most significant effects on the detection and detection performance of the sensor. For example, more mission time is required to achieve full coverage of the intended area if the cross-track detection range of the sonar is reduced due to environmental conditions. The ability to estimate accurately the sensor performance in challenging seabed conditions is still difficult to achieve, especially in high cluttered environments. Note that there is current work on modeling of the seabed, Myers 2005.

However, in this first attempt to analyze the effectiveness of AUVs, we assume a benign seabed condition with high target-strength mines. Reasonable assumptions can be made about the sensor performance in this case. That is, the probability of calling a mine as a mine is very high (approximately 100 percent) while the probability of calling a non-mine as a mine is very low (approximately zero percent). Table 2 shows all the possible outcomes of an observation of an object lying on the seabed. The diagonal cells in Table 2 have a probability close to 100 percent. For simplicity, we further assume that all mines are cylindrical.

Table 2. *Operator decisions*

	OPERATOR PERCEPTION	
TRUE STATES	***With mines***	***No mines***
With mines	P_m	$1 - P_m$
No mines	P_f	$1 - P_f$

2.2 Challenges

Before we introduce the concepts of operations, we will first define the coordinate system to help clarify the notations. Fig. 3 defines the coordinate system where x is the horizontal axis and y is the vertical axis. The blue lines represent the AUV path while the red circles are mines and the interior of the rectangle frame is the search area. The arrow in the search area indicates the general direction of the AUV. The vehicle starts at the bottom left, then travels from left to right, then travels upward, then travels right to left, then travels upwards and repeats.

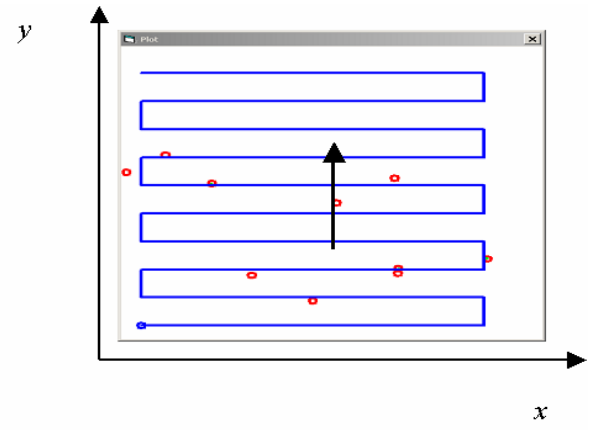

Figure 4. *Coordinate system*

The AUV path shown in Fig. 3 is a typical search pattern called the lawn mowing pattern or the creeping line of advance. Each search pattern is characterized by its measures of effectiveness (MOEs). These MOEs may include the probability of detection, coverage, overlap and search time. They can be determined using the geometry of the scenario and the measures of performance (MOPs) of the sonar.

2.2.1 Measures of performance

To assess the effectiveness of MCM operations, we need to understand the sonar Measures Of Performances (MOPs): the probability of detection as a function of range as shown in Fig. 4 and the probability of detection as a function of aspect angle as shown in Fig. 5. Note that the aspect angle is defined as the angle between the sonar beam and the axis of symmetry of a cylindrical mine. We assume that these two probabilities are independent. The probability of detection as a function of range is assumed to be primarily a characteristic of the side scan sonar while the probability of detection as a function of angle is assumed to be primarily a characteristic of the mine. These probability curves are modelled using the Johnson distribution (1) as it is fairly versatile in the sense that we can make it unimodal or bimodal, skewed to the left, symmetric, or skewed to the right as well as controlling how narrow each peak is, Law and Kelton 2000. The scale (λ) shown below is a factor compounded to Johnson's distribution such that the maximal value of each curve is equal to 1.

The Johnson's curve can be expressed as:

$$f(x) = \begin{cases} \dfrac{\lambda \cdot \alpha_2 \cdot (x_2 - x_1)}{(x - x_1) \cdot (x_2 - x) \cdot \sqrt{2\pi}} e^{-\frac{1}{2}\left(\alpha_1 + \alpha_2 \cdot \ln\left(\frac{x - x_1}{x_2 - x}\right)\right)^2} & x_1 < x < x_2 \\ 0 & \text{otherwise} \end{cases} \tag{1}$$

The range probability curve shows that at very close ranges and ranges near the maximum range the probability of detection drops from close to 100 percent to zero percent. The angular probability curve shows that the detection of the mine reaches a maximum when its aspect angle is perpendicular to the side scan sonar beam and this angular probability is decreased symmetrically with respect to that perpendicular case.

Table 3. *Johnson parameters defining the range and angle probability curves*

	JOHNSON'S PARAMETERS	
Range probability curve	$\alpha_1 = 0$, $\alpha_2 = 0.75$	$x_1 = 11.5\,\text{m}$, $x_2 = 75\,\text{m}$
Angle probability curve	$\alpha_1 = 0$, $\alpha_2 = 1.25$	$x_1 = 0$, $x_2 = \pi$

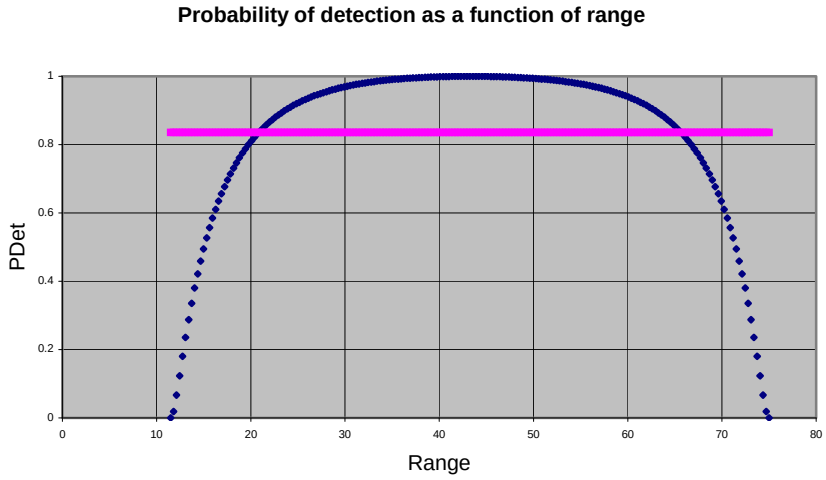

Figure 5. *Probability of detection as a function of range*

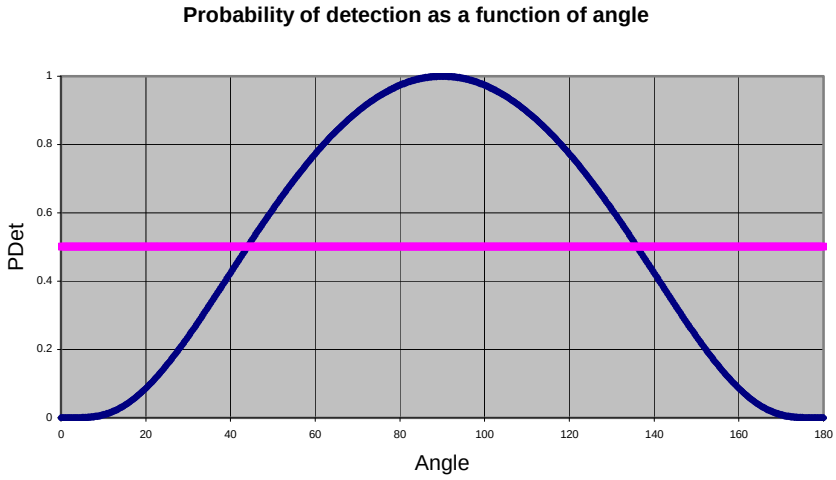

Figure 6. *Probability of detection as a function of angle*

It is very clear from Fig. 5 that the probability of detection is substantially degraded if the aspect angle differs from 90 degrees. The impact of this degradation is shown in Fig. 6 and Fig. 7. In Fig. 6, a mine is observed at an angle of 85 degrees while, in Fig. 7, the same mine is observed at an angle of 0 degrees. The mine is without a doubt identified in Fig. 6 by an experienced operator. However, the same mine in Fig. 6 is very difficult to recognize when viewed at an aspect angle of 0 degrees, as shown in Fig. 7.

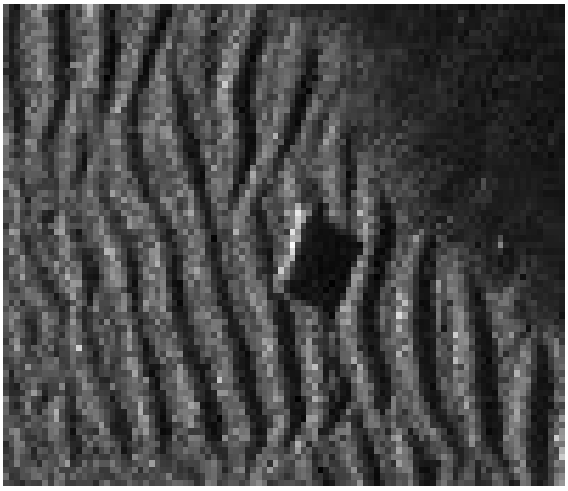

Figure 7. *Mine observed at 85 degrees*

Figure 8. *Mine observed at 0 degrees*

3. Preliminary analysis

Assuming that the spacing between two consecutive horizontal legs of the lawn mowing search pattern shown in Fig. 3 is typically equal to twice the maximal range of detection, implies that the probability of detection obtained by the lawn mowing search pattern is approximately 40 percent. This is so as the mean range probability of detection is about 80 percent (Fig. 4) while the mean angular probability of detection is about 50 percent (Fig. 5). The product of the twos is equal to 40 percent.

Fig. 8 displays the coverage and the probability of detection as a function of search time for the lawn mowing pattern. Note that an increase in search time represents an increase in number of long (horizontal in this case) legs in the search pattern. Fig. 8 shows a large difference between the coverage and the probability of detection. This degradation is due mainly to the low mean value of the angular probability of detection as alluded above.

In addition, Fig. 8 shows that both the coverage and the probability of detection decrease as a function of search time when the search time is approximately between six and nine hours for the lawn mowing pattern. Why is that so? This is not an error. It is due to the fact that as search time increases the spacing between the horizontal legs in Fig. 9 decreases.

Associated with each long leg there is a gap due to the minimal range of detection of the sonar. Initially, as we increase the number of legs, the overall coverage increases proportionately. However, at some point the maximum ranges of two abutting legs will touch, resulting in a certain coverage. At this point, as the additional legs introduce additional gaps, while the coverage from abutting legs simply overlap each other. These additional gaps result in a small decrease in coverage as time increases until the point when abutting legs start to fill in each others gap. At this point, the overall coverage starts to increase again, until eventually all of the gaps are covered and the coverage is 100 percent. This suggests that simply increasing the number of legs in a lawn mowing pattern is not an effective technique since the MOEs do not improve as a function of investment in search time.

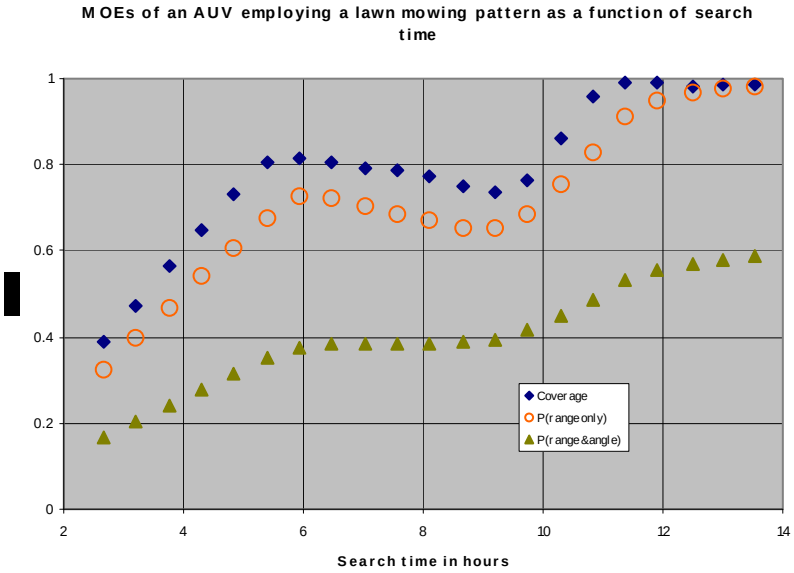

Figure 9. *MOEs of an AUV employing a lawn mowing pattern as a function of search time*

In summary, the usual lawn mowing pattern poses two problems. First, the MOEs do not always improve as a function of search time due to the gap in detection range. Second, there is a fundamental limitation in the probability of detection for a search pattern with a single search angle. The solutions to these two issues are presented in the next section.

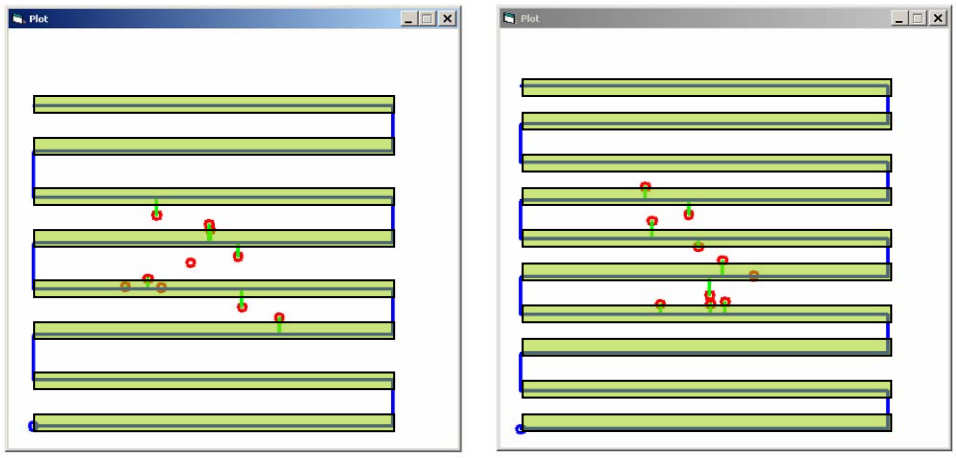

Figure 10. *Anomaly due to the minimal detection range*

4. Concepts of operations

4.1 Gaps in coverage

If the AUV conducts an uneven mowing pattern, as shown in Fig. 10, then it will eliminate gaps in coverage. This search pattern is designed to provide 100 percent coverage of the search area, in addition to minimizing overlaps and search time with respect to other mowing paths. With that in mind, we derive that the small spacing between horizontal legs must be equal to the maximal detection range subtracted by the minimal detection range $(r_{\max} - r_{\min})$ while the large spacing between them must be equal to twice the maximal detection range $(2 \cdot r_{\max})$. Note that this solution can be fulfilled only if $r_{\max} \geq 3 \cdot r_{\min}$, a condition that is met by the parameters shown in Table 3.

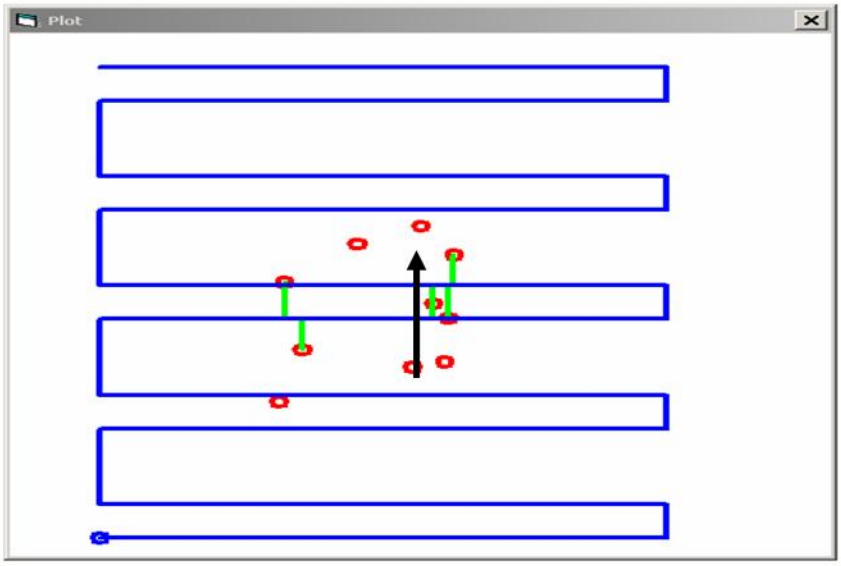

Figure 11. *Uneven lawn mowing pattern*

4.2 Aspect angle degradation

The degradation due to the angular probability of detection, described in the previous section can be reduced by fusing more than one observation of a mine at different aspect angles, Zerr etal. 2000; Nguyen and Hopkin 2005a, b. Fig. 11 displays a cylindrical mine (in green) observed from two angles: 30 degrees and 60 degrees. The fusion of these two observations improves the angular probability of detection by six percent based on the probability curve shown in Fig. 5. We can understand this improvement by observing that the angular probability of detection by the first AUV leg is $P_1 = 77$ percent while the angular probability

of detection by the second AUV leg is equal to $P_2 = 24$ percent. Combining the two results of the two AUV legs, the angular probability of detection becomes $P_{1-2} = 1-(1-P_1)(1-P_2) = 83$ percent – an improvement of six percent with respect to $P_1 = 77$ percent.

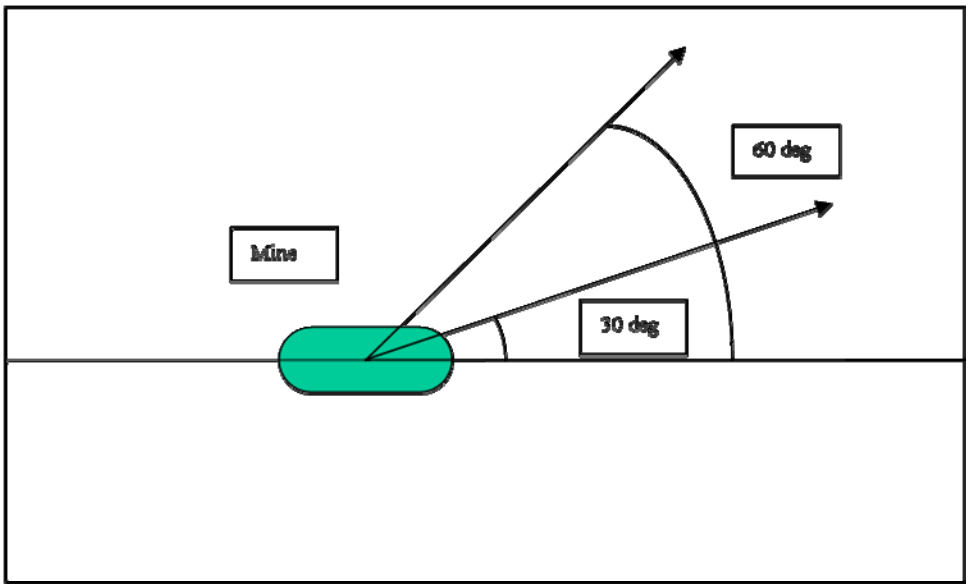

Figure 12. *Mine aspect angles*

4.2.1 Optimality with two different angular observations

If an AUV can observe a same mine from two different angles then it is natural to ask how the two angles should be related to one another such that the angular probability of detection is optimal. Fig. 12 sheds light on this question. P_1 represents the mean angular probability of detection generated by one AUV leg while $P_2(\phi)$ represents the mean angular probability of detection generated by two AUV legs plotted as a function of angle ϕ between them. Fig. 12 shows that $P_2(\phi)$ is better than P_1 and in addition $P_2(\phi)$ achieves a maximum when $\phi = 90^o \left(\frac{\pi}{2}\right)$. That is, to maximize the angular probability of detection with two observations at two different angles, the difference between the two angles must be $90^o \left(\frac{\pi}{2}\right)$.

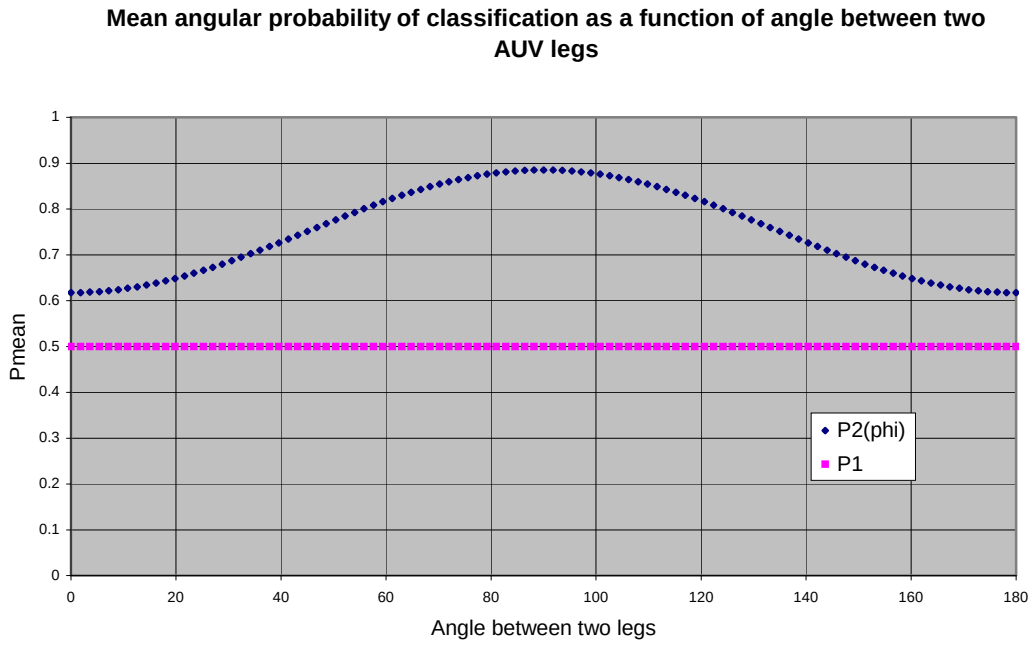

Figure 13. *Mean angular probability of classification as a function of angle between two AUV legs*

The proof of this assertion is described below. However, for the purpose of this section, it is convenient to redefine the aspect angle θ by shifting it to the left by $90\,\text{deg}$ such that the maximal angular probability of detection occurs at $0\,\text{deg}$.

To obtain P_1 and P_2, we assume that a mine lies between the minimal and maximal range of an AUV leg and two AUV legs respectively. P_1 is computed by integrating the angular probability of detection, shown in Fig. 3, from $-90\,\text{deg}\left(-\frac{\pi}{2}\right)$ to $+90\,\text{deg}\left(\frac{\pi}{2}\right)$ and then averaging it through a division by $180\,\text{deg}(\pi)$. P_2 is computed in the same way with the exception that it is based on two AUV legs whose relative angle is ϕ.

$$P_1 = \frac{1}{\pi} \cdot \int_{-\frac{\pi}{2}}^{\frac{\pi}{2}} d\theta \cdot f(\theta) \tag{2}$$

$$P_2(\phi) = 1 - \frac{1}{\pi} \cdot \int_{-\frac{\pi}{2}}^{\frac{\pi}{2}} d\theta \cdot \left(1 - f(\theta)\right) \cdot \left(1 - f(\theta + \phi)\right) \tag{3}$$

where $f(\theta)$ is the Johnson function whose parameters are defined in Table 3. The fact that P_2 reaches a maximum at $\phi = 90\,\text{deg}$ is true in general. It is due to the shape and symmetry of the angular probability of detection curve. Fig. 13 displays the angular probability of

detection $f(\theta)$ in blue and its first derivative at $\phi = 90\,\text{deg}$, $\left.\frac{d}{d\phi} f(\theta+\phi)\right]_{\phi=\frac{\pi}{2}}$ in purple as a function of redefined angle θ.

Observe that the derivative of $P_2(\phi)$ at $\phi = 90\,\text{deg}$ is:

$$\left.\frac{d}{d\phi} P_2(\phi)\right]_{\phi=\frac{\pi}{2}} = \frac{1}{\pi} \cdot \int_{-\frac{\pi}{2}}^{\frac{\pi}{2}} d\theta \cdot (1 - f(\theta)) \cdot \left.\frac{d}{d\phi} f(\theta+\phi)\right]_{\phi=\frac{\pi}{2}} \tag{4}$$

Fig. 13 shows that $f(\theta)$ is an even function of θ. Thus, $1 - f(\theta)$ is also an even function of θ. In addition, $\left.\frac{d}{d\phi} f(\theta+\phi)\right]_{\phi=\frac{\pi}{2}}$ is an odd function of θ. Hence, the integrand of equation (4) is odd at $\phi = 90\,\text{deg}\left(\frac{\pi}{2}\right)$ implying that $\left.\frac{d}{d\phi} P_2(\phi)\right]_{\phi=\frac{\pi}{2}} = 0$. Therefore, $P_2(\phi)$ achieves an optimum at $\phi = 90\,\text{deg}\left(\frac{\pi}{2}\right)$. Appendix A further shows that this is not only an optimum but in fact it is a global maximum.

This optimality condition corresponds to the employment of two AUVs where each conducts a lawn mowing pattern perpendicularly to one another as shown in Fig. 14.

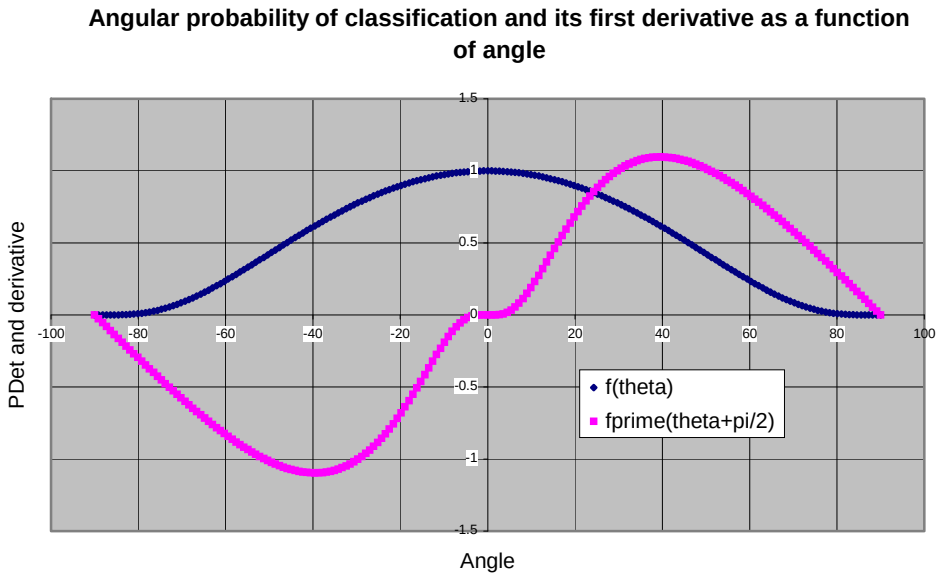

Figure 14. *Angular probability of classification and its first derivative as a function of angle*

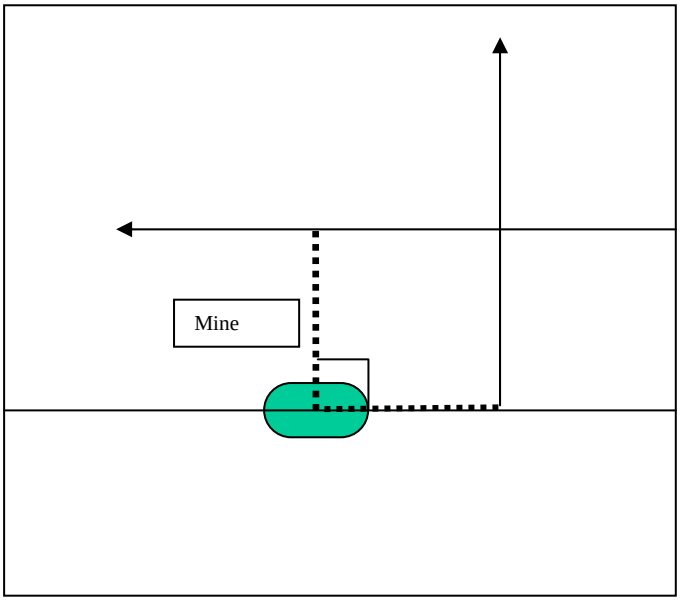

Figure 15. *Two perpendicular observations of a same mine*

4.2.2 Optimality with N different angular observations

It turns out that we can generalize the result in the previous subsection. That is, we are able to determine the angles such that the angular probability of detection is optimal when a mine is observed N times from the same range. We show that if $\phi_i = i \cdot \varphi$ where $i = 0..N-1$ and $\varphi = \frac{\pi}{N}$ then the resulting mean angular probability of detection is maximal. For example, if there are three angular observations then the mean angular probability of detection is maximal when $\phi_0 = 0; \phi_1 = \pi/3; \phi_2 = 2\pi/3$.

To prove this assertion, we only need to show that $\left(\frac{\partial}{\partial \phi_0} P_N\left(\vec{\phi}\right)\right)_{\phi_i = i\cdot\theta} = 0$ since we can always choose a coordinate system that is rotated in a way such that for any i, ϕ_i becomes zero. $\left(\frac{\partial}{\partial \phi_0} P_N\left(\vec{\phi}\right)\right)_{\phi_i = i\cdot\theta}$ can be expressed as:

$$\left(\frac{\partial}{\partial \phi_0} P_N\left(\vec{\phi}\right)\right)_{\phi_i = i\cdot\theta} = \int_{-\frac{\pi}{2}}^{\frac{\pi}{2}} \frac{d\theta}{\pi} \cdot g'(\theta) \cdot g(\theta+\varphi) \cdot \ldots \cdot g\left(\theta + (N-1)\cdot\varphi\right) \tag{5}$$

The above is zero if $g'(\theta)$ is odd and $g(\theta+\varphi)\cdot g(\theta+2\cdot\varphi)\cdot\ldots\cdot g\left(\theta+(N-1)\cdot\varphi\right)$ is even as this implies that the integrand is odd. And integrating an odd function from $-\pi/2$ to $\pi/2$ gives zero.

Since $g(\theta)$ is even, we infer that $g'(\theta)$ is odd. Moreover,

$$\begin{aligned}
&g(-\theta+\varphi)\cdot g(-\theta+2\cdot\varphi)\cdot\ldots\cdot g\left(-\theta+(N-1)\cdot\varphi\right)\\
&= g(\theta-\varphi)\cdot g(\theta-2\cdot\varphi)\cdot\ldots\cdot g\left(\theta-(N-1)\cdot\varphi\right)\\
&= g(\theta-\varphi+N\cdot\varphi)\cdot g(\theta-2\cdot\varphi+N\cdot\varphi)\cdot\ldots\cdot g\left(\theta-(N-1)\cdot\varphi+N\cdot\varphi\right)\\
&= g\left(\theta+(N-1)\cdot\varphi\right)\cdot g\left(\theta+(N-2)\cdot\varphi\right)\cdot\ldots\cdot g(\theta+\varphi)
\end{aligned}$$

The first equality is true due to the fact that $g(\theta)$ is even. The second equality is true due to the fact that $g(\theta)$ is periodic with a period equals to $N\cdot\varphi = \pi$. The last equality shows that the product is an even function. Hence the integrand of equation (5) is odd and thus the integral is zero.

5. Modelling and algorithm

Now that we have found a solution that eliminates gaps in coverage and improves the detection performance by fusing multiple target aspect angles, we implement this solution in a Monte Carlo model and a deterministic model of mission effectiveness. The Monte Carlo model is coded in Visual Basic (VB) while the deterministic model is coded in MathCad. These two models are distinct but equivalent. They allow validation of the measures of effectiveness by comparing those from the Monte Carlo simulation to those obtained by the deterministic model. The MOEs may include:

a. Search time.

b. Probability of detection.

c. Detection rate defined as the ratio of the probability of detection to the search time.

d. Coverage (the percentage of the search area that lies between the minimal and maximal range of the AUV path).

The above list is by no means exhaustive but they are representative of the effectiveness of a mine hunting mission. Depending on the mandate, we can assign different priorities to the above MOEs. For instance, if the searcher is limited in time then he might want to maximize the detection rate. Doing so will give him the highest probability of detection in a fixed time. However, if the search area is to be sanitized, then the searcher will do his best to maximize the probability of detection. This can be done by searching the area exhaustively to maximize coverage, and deploying more than one AUV with distinctive paths to maximize the angular probability of detection.

5.1 Monte Carlo simulation

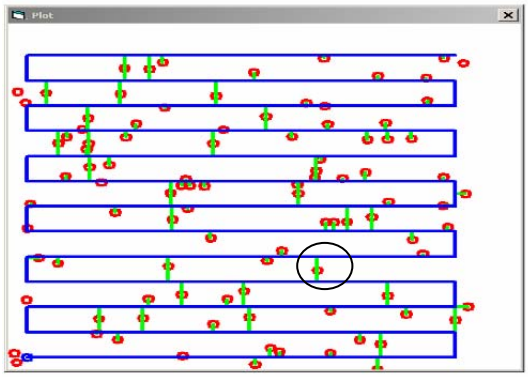

Figure 16. *Stochastic simulation*

The underlying algorithm is shown in Fig. 15. For each run, the AUV employs the same search path (blue lines) while the positions (red circles) and angles (not shown) of the mines are generated based on an a priori distribution. If a mine lies between the minimal and maximal range of the AUV then a green line is drawn connecting that mine to the AUV. When multiple AUV legs cover a same mine, a green line is drawn from each leg to that mine e.g. the mine laying inside the black circle is covered by two legs, one above and one below. The simulation then computes the probability of detection using the range probability curve and the angular probability curve. It also fuses data when a same mine is detected by more than one leg and/or more than one AUV as discussed earlier.

The program collects the results of each run, performs the statistics and outputs the measures of effectiveness. This simulation has the advantage that it displays the dynamics of the search paths, which is useful when planning for an experimental design.

We make use of the Chernoff's bound, Chernoff 1952, to determine the number of Monte Carlo runs (m) required to achieve a given accuracy (ε) and a pre-determined confidence level $(1-\delta)$:

$$m \geq \frac{1}{2 \cdot \varepsilon^2} \cdot \ln\left(\frac{2}{\delta}\right)$$

This criterion implies that:

$$P\left(\left|\hat{P} - P_T\right| \leq \varepsilon\right) = 1 - \delta$$

where $\hat{P}$ is the estimated probability collected from the Monte Carlo simulation of m runs while P_T is the true probability. As an example, to meet a 5 percent accuracy and a 95 percent $(\delta = 0.05)$ confidence level, we need 738 runs.

5.2 Deterministic model

The search area is divided into a grid consisting of 200 by 200 cells. For each cell and for each leg of the AUVs, we determine whether that cell lies between the minimal and maximal range of detection of that AUV leg. If it does then we compute the probability of detection using the probability curves and the probability density of the mine.

For example, if the mines are uniformly random in the search area then the probability density of a cell is equal to the area size of the cell divided by the size of the search area. The corresponding contribution of each cell to the total probability of detection is simply equal to $(\Delta \cdot P_g / A)$ where A is the size of the search area while Δ is the size of the cell and P_g is the probability of detection of that cell based on range, aspect angle and the AUVs search path. This probability P_g can be expressed as $P_g = 1 - \prod_{i=1}^{d} (M_i)$ where d is the number of AUV legs whose coverage contain that cell, and $M_i (\leq 1)$ is the probability that the ith leg misses the same cell. In general, as d increases then so is P_g.

5.3 Validation

Fig. 16 also reveals that P(deterministic) and P(stochastic) are virtually identical. P(deterministic) is obtained from the deterministic model. It is essentially a triple integral over the search area and over the aspect angle of the mine. P(stochastic) is obtained from running the stochastic simulation 100 times and then collecting the statistics. This shows that our calculations are consistent since the two models are equivalent and yet are designed differently. In what follows, we will refer to P as the probability of detection: one that accounts for both range and aspect angle.

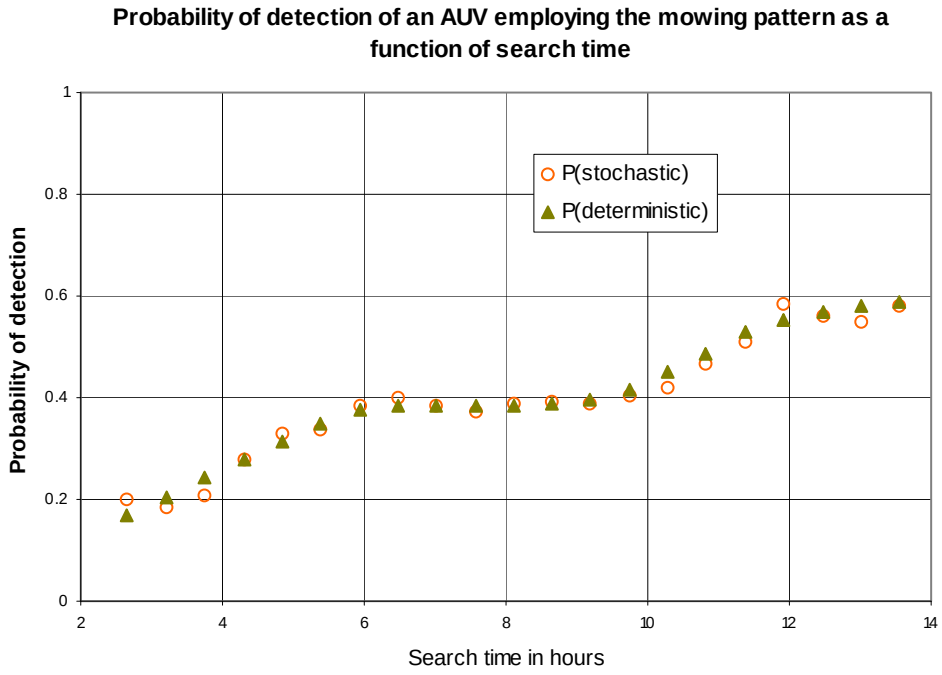

Figure 17. *Comparing the results of the stochastic simulation to those of the deterministic model*

5.4 Random search formula adapted to AUVs

Before we present the results of the models described above, we will derive a formula for the probability of detection of an AUV conducting a random search. This formula will allow comparison in the effectiveness between a random search and the novel concept of operations proposed for the AUVs. Since the side-scan-sonar MOPs (Fig. 4 and Fig. 5) indicate that the detection probability is not perfect in general and in fact, it depends on both range and angle, it is clear that we need to modify Koopman's formula, Koopman 1999, to determine the detection probability of an AUV conducting random search operations. Fortunately, this modification is simple and so we will present the derivation below.

We divide this search length into n search segments each of which has a length of L/n. The maximal detection range $r_{\max}$, the minimal detection range $r_{\min}$ and the length of each search segment cover two small rectangles, Fig. 17.

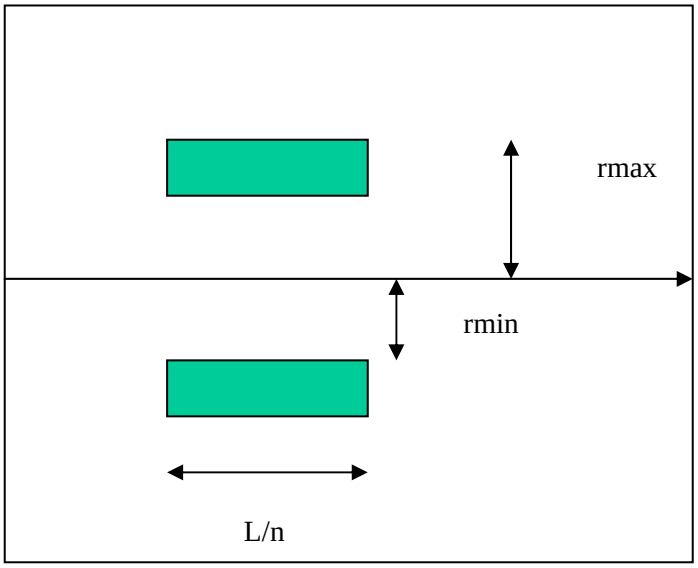

Figure 18. *Coverage of* L/n *search segment*

Based on a uniform density distribution, the probability of detection of a mine lying in this sub area is equal to:

$$p_K(\theta) = \frac{L}{n} \cdot \frac{2 \cdot \int_{r_{\min}}^{r_{\max}} p(r) \cdot dr}{A} \cdot p(\theta)$$

where $p(r)$ is the detection probability as a function of range (r) as shown in Fig. 4 while $p(\theta)$ is the detection probability as a function of angle (θ) as shown in Fig. 5 and K stands for Koopman. In a random search, this angle θ is uniformly random. This is so as the AUV changes its course randomly for a given mine with a fixed orientation.

The above result can be further simplified by recalling that the detection probability as a function of range was modeled as a Johnson's density distribution scaled by λ_r as defined in equation(1):

$$\int_{r_{\min}}^{r_{\max}} p(r)\cdot dr = \int_{r_{\min}}^{r_{\max}} f(r)\cdot dr = \lambda_r \cdot \int_{r_{\min}}^{r_{\max}} f_J(r)\cdot dr = \lambda_r$$

The probability that a mine lies in the sub area can now be written as:

$$p_K(\theta) = \frac{(L/n)\cdot 2\cdot \lambda_r}{A}\cdot p(\theta)$$

The probability that a mine lies outside of this rectangle is simply:

$$q_K(\theta) = 1 - p_K(\theta)$$

The only way that the AUV misses a mine after n independent and random search segments, is to miss it in every search segments. As a result, the detection probability due to n search segments is equal to:

$$P_K = 1 - \left(\prod_{i=1}^{n}\left(q_K(\theta_i)\right)\right)^n = 1 - \prod_{i=1}^{n}\left(1 - \frac{2\cdot\lambda_r\cdot(L/n)}{A}\cdot p(\theta_i)\right)$$

Expanding the product:

$$\begin{aligned} P_K &= 1 - \left(1 - \frac{L\cdot 2\cdot\lambda_r}{n\cdot A}\cdot\sum_{i=1}^{n} p(\theta_i) + \ldots\right) \\ &= 1 - \left(1 - \frac{L\cdot 2\cdot\lambda_r}{A\cdot\pi}\cdot\frac{\pi}{n}\sum_{i=1}^{n} p(\theta_i) + \ldots\right) \\ &= 1 - \left(1 - \frac{L\cdot 2\cdot\lambda_r}{A\cdot\pi}\cdot\int_0^{\pi} d\theta\cdot p(\theta) + \ldots\right) \end{aligned}$$

The key argument in the above equation is the third equality. The sum in the second equality can be sorted in increasing order of θ_i. As θ is uniformly random, for large n, $\theta_i = i\cdot\frac{\pi}{n}$ after sorting. This sum compounded to $\frac{\pi}{n}$ is exactly $\int_0^{\pi} p(\theta)\cdot d\theta$. Again, recalling that $p(\theta)$ was modeled as a Johnson's density distribution scaled by λ_θ, we get $\int_0^{\pi} p(\theta)\cdot d\theta = \lambda_\theta$. Taking the limit as n tends to infinity yields the following formula, Zwillinger 1996:

$$\begin{aligned} P_K &= 1 - \left(1 - \frac{L\cdot 2\cdot\lambda_r\cdot\lambda_\theta}{A\cdot\pi} + \ldots\right) \\ &= 1 - \left(1 - \frac{L\cdot 2\cdot\lambda_r\cdot\lambda_\theta}{n\cdot A\cdot\pi}\right)^n \\ &= 1 - e^{-\left(\frac{2\cdot\lambda_r\cdot L}{A}\cdot\frac{\lambda_\theta}{\pi}\right)} \\ &= 1 - e^{-\left(\frac{2\cdot\lambda_r\cdot V\cdot t}{A}\cdot\frac{\lambda_\theta}{\pi}\right)} \end{aligned} \qquad (6)$$

P_K is the probability of detecting a mine by an AUV conducting a random search. This formula has an attractive interpretation. The detection range R is replaced by an effective range $R_{effective} = \lambda_r$ due to two characteristics of the probability of detection as a function of range. First, there is a minimal detection range i.e. if a mine is observed at a range less than the minimal detection range then it will not be detected. Second, detection is not perfect for a mine lying between the minimal and maximal ranges. Hence, the original detection range is replaced by an effective detection parameter λ_r. For example, in our scenario the minimal detection range is 11.5 m while the maximal detection range is 75.0 m. This generates an effective detection range λ_r of approximately 53.06 m.

Additionally, the power of the exponential is multiplied by $\frac{\lambda_\theta}{\pi}$ which represents the mean angular probability of detection. In our scenario, the effective angular range, λ_θ, is approximately 90 deg implying a mean angular detection probability of approximately 50 percent. This modification is essential as Koopman's original formula assumes no angular dependence. That is, the probability of detection as a function of angle is 100 percent in Koopman's original derivation.

In the case of more than one AUV, the same formula can be used with the exception that the power to the exponential term has to be multiplied by the number of AUVs. The reason for this is simple: each AUV conducts a random search means that the motions of two AUVs say are completely independent. This is equivalent to having one AUV executing a random search for twice the amount of search time. Therefore, in general the probability of detection of a identical AUVs can be expressed as:

$$P_K(a) = 1 - e^{-\left(\frac{2 \cdot a \cdot \lambda_r \cdot V \cdot t}{A} \frac{\lambda_\theta}{\pi}\right)} \tag{7}$$

6. Mine countermeasure exploratory operations

This experiment is an experiment to test mine exploratory operation concept. The search area is divided into a total of N sub areas or cells. Each cell is a square, has a same size and contains at most one mine. For the sake of simplicity, we assume that there is a uniformly random probability of having n mines in the search area where n ranges from zero to N, that is $p(n) = 1/N$. This choice is arbitrary and can be replaced by any other density distributions. It also does not affect the derivation below. These n mines are further distributed randomly among the N cells. The objective of the experiment is to determine the resources required in order to establish the presence or absence of mines in the search area.

The resources are measured in terms of the number of cells that are fathomed, denoted as m. When searching m sub areas, there is a probability that m_d of these sub areas have mines and the remaining $m_a = m - m_d$ have no mines. The probability associated with such an event belongs to a hypergeometric density distribution:

$$P_{m_d, m_a} = \frac{\binom{n}{m_d} \cdot \binom{N-n}{m_a}}{\binom{N}{m = m_d + m_a}} \tag{8}$$

There are two outcomes from a search in a cell with a mine: detected or not detected. Assuming there is a mine, the probability of detection is denoted as P_d while the probability of non-detection is denoted as Q_d where d stands for detection. There are also two outcomes from a search in a cell with no mines: false alarm and no false alarm. Assuming there is no mine, the probability of a false alarm is denoted as P_a while the probability of a non false alarm is denoted as Q_a where a stands for alarm. Combining the detection probability and the false alarm probability of each sub area to the hypergeometric density distribution, we obtain the probability of finding at least an object that looks like a mine:

$$P_e = \frac{1}{N} \cdot \sum_{n=0}^{N} \left(1 - \sum_{m_d + m_a = m} P_{m_d, m_a} \cdot (Q_d)^{m_d} \cdot (Q_a)^{m_a} \right) \tag{9}$$

As this is a first attempt to analyze exploratory operations, we have picked an area where the environment is benign. That is, $Q_a = 1$. Therefore, in this scenario, the probability of finding at least a mine is equal to:

$$P_e = \frac{1}{N} \cdot \sum_{n=0}^{N} \left(1 - \sum_{m_d + m_a = m} P_{m_d, m_a} \cdot (1 - P_d)^{m_d} \right) \tag{10}$$

7. Numerical results

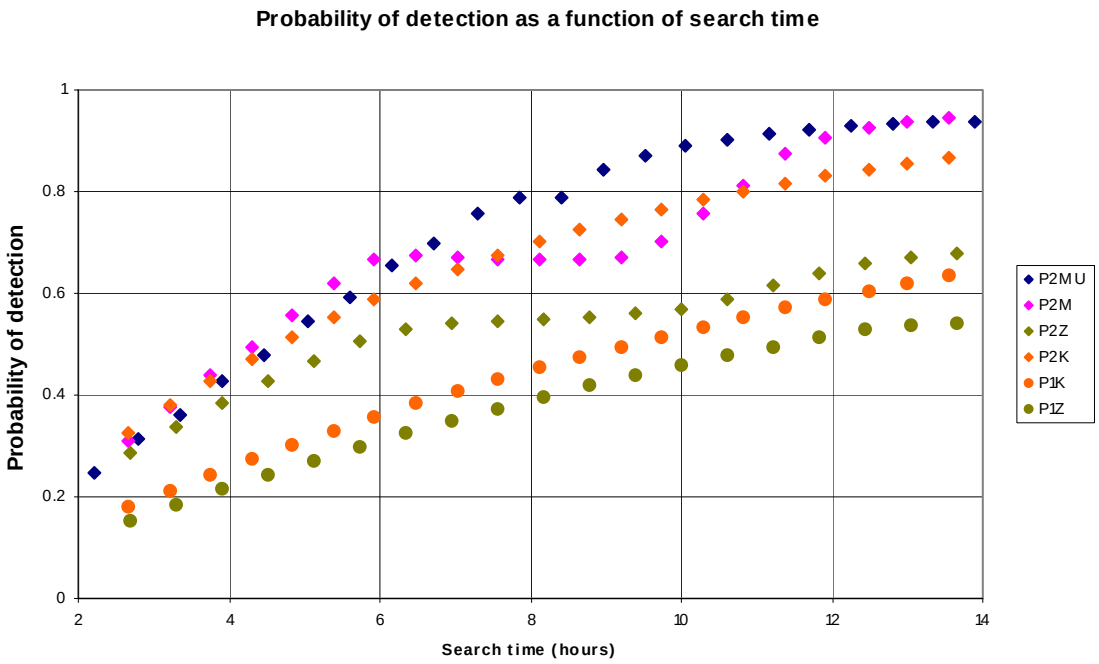

Figure 19. *Probability of detection as a function of search time*

Fig. 18 compares the probability of detection among the search patterns. P2MU corresponds to two perpendicular uneven lawn mowing pattern, Fig. 19; P2M corresponds to two perpendicular regular lawn mowing pattern, Fig. 20; P2Z corresponds to two complementary zigzag search patterns & P1Z corresponds to the zigzag search pattern, Fig. 21, and P2K corresponds to a random search pattern conducted by two AUVs. For completeness, we also show the search pattern of one AUV conducting the uneven lawn mowing pattern and the regular lawn mowing pattern, Fig. 19 and Fig. 20 respectively.

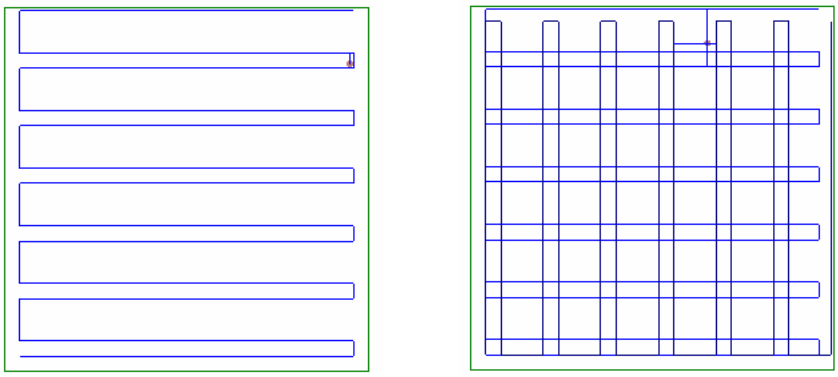

Figure 20. *Uneven lawn mowing patterns*

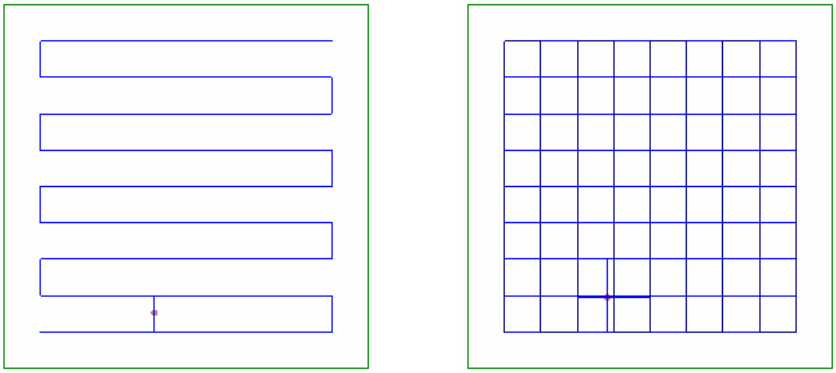

Figure 21. *Regular lawn mowing patterns*

Fig. 18 shows that P2MU is the best and can be similar to P2M. However, unlike P2M, P2MU is monotonically increasing as a function of investment in search time, an indication that the uneven lawn mowing pattern is consistent. There is a large difference between P2MU and P2Z, approximately 40 percent at search time equals to 14 hours, due to the angular optimality of perpendicular search patterns as proved earlier. P1Z is representative of the zigzag search pattern conducted by one AUV as well as the uneven mowing pattern and the regular mowing pattern since the probability of detection based on one AUV is very similar for these search patterns.

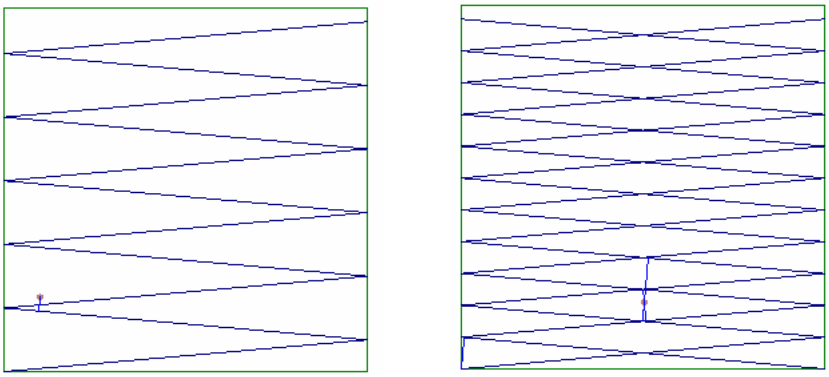

Figure 22. *Zigzag patterns*

Note that P2K is similar to P2MU as a random search can detect a same mine at many different angles, improves the angular probability of detection and the overall probability of detection substantially. For the same reason, P1K is better than P1Z. In practice, an AUV can not conduct a random search as it requires a straight line search segment to collect data while a random search necessitates that the AUV changes its direction continuously. Nevertheless, it is possible in theory to allow the AUV to collect data for a fixed time period, say 15 minutes, and then changes its course randomly. Doing so will decrease P2K. For the sake of argument, let's assume that the AUV spends half the time collecting data on straight line segments and the other half turning his direction randomly, this implies that the AUV is effective only half of the time and therefore $P2K = P_K(2)$ becomes $P_K(1) = PK1$. In light of this information, Fig. 18 shows that the 2MU search pattern achieves better effectiveness than that of a random search, another indication that 2MU is the right search pattern to be employed.

Fig. 22 displays the rate of detection as a function of search time. For clarity, we show only the rates of detection for the uneven lawn mowing pattern and for the zigzag search pattern. Again, the uneven lawn mowing pattern provides better results than those of the zigzag pattern.

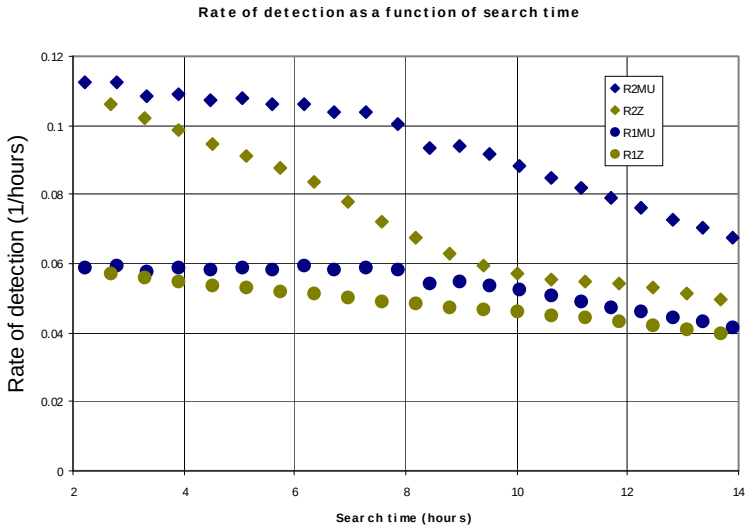

Figure 23. *Rate of detection as a function search time*

Fig. 23 shows the probabilities of detecting at least a mine as a function of number of searched cells. We pick the same search time of 8 hours for each cell and for each search pattern. The values of the probabilities of detection are obtained from Fig. 18 and are displayed in Table 4.

Fig. 23 shows that P2MUe is the best among the four scenarios. This improvement is most significant for number of searched cells less than six $(m \le 6)$. Such an improvement helps reduce resource and time requirements in conducting mine countermeasure operations. For instance, a 2Z search pattern takes at least 48 hours (searching 6 cells), to achieve the same probability of detecting at least a mine, as a 2MU that takes 32 hours (searching 4 cells). Equivalently, the difference between the probability of detecting at least a mine after searching 6 cells based on the 2Z search pattern and that based on the 2MU search pattern is more than 10 percent, a substantial improvement in the confidence of finding at least a mine. This shows the importance of choosing the right search pattern.

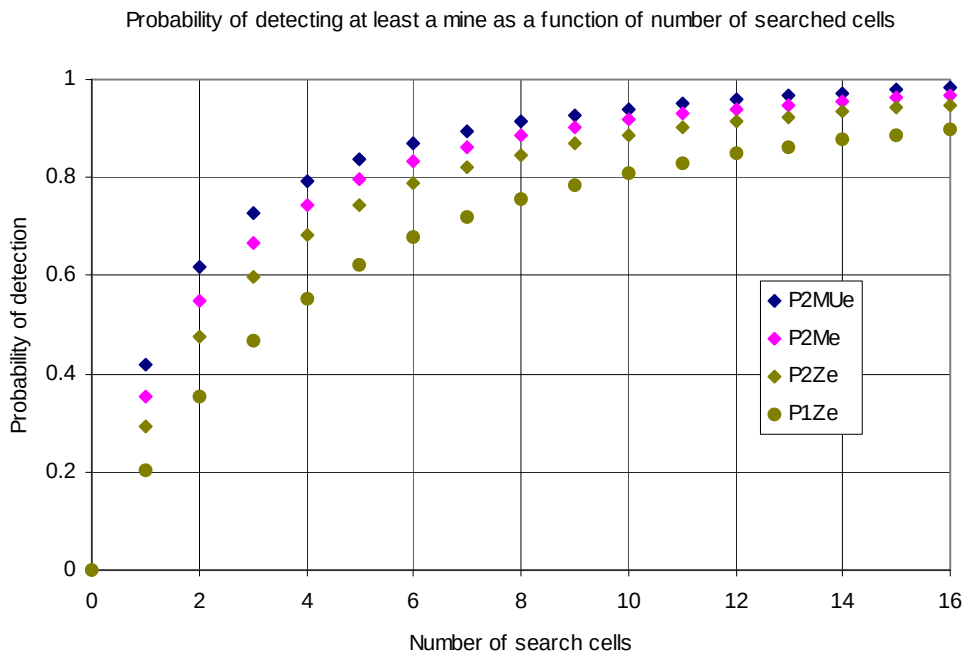

Figure 24. *Probability of detecting at least a mine as a function of search time*

Table 4. *Probability of detection for a search time equals to 8 hours*

SEARCH PATTERN	OPERATOR PERCEPTION
2MU	0.79
2M	0.67
2Z	0.55
1Z	0.39
2K	0.70
1K	0.45

8. Conclusions

In this paper, we have examined a number of search patterns: lawn mowing, zigzagging and random searches. The measures of effectiveness of the first two patterns were evaluated through the use of a stochastic and a deterministic model whose outcomes were shown to be consistent.

Based on the assumed measures of performance, we showed that the two AUVs conducting perpendicular uneven mowing patterns (2MU search pattern) provides the best probability of detection as a function of search time. This optimality is due to two features. First, the uneven mowing pattern is designed so that there are no gaps between consecutive legs. Second, two perpendicular search patterns maximizes the angular probability of detection as proved in the main text and in more details in Annex A.

We have also shown how the search pattern impacts on time and resource requirements for mine countermeasure exploratory operations.

9. References

1. Chernoff Herman. A measure of asymptotic efficiency for tests of a hypothesis based on the sum of observations. Ann. Math. Stat, 1952, vol. 23, pp. 493-507.

2. Gelfand I. M. and S. V. Fomin. Calculus of Variations. 13th edition, Prentice-Hall, 1964, p 19.

3. Koopman B. O.. Search and Screening: General Principles with Historical Applications. The Military Operations Research Society Inc., 1999, pp. 71-74.

4. Law Averill M. and W. David Kelton. Simulation Modeling and Analysis. 3rd edition, McGraw-Hill series in industrial engineering and management science, 2000, pp. 314-315.

5. Myers Vincent, private communication, NATO Undersea Research Centre, 16 Mar 2005.

6. Nguyen Bao and David Hopkin. Modelling Autonomous Underwater Vehicles (AUVs) in Mine Hunting. IEEE Oceans 05 Conference Proceedings, 20-23 Jun 2005, Brest, France.

7. Nguyen Bao and David Hopkin. Concepts of Operations for the Side Scan Sonar Autonomous Underwater Vehicles Developed at DRDC Atlantic, Technical Memorandum TM 2005-213, October 2005.

8. Zerr B., E. Bovio and B. Stage. Automatic Mine Classification Approach Based on AUV Manoeuvrability and COTS Side Scan Sonar. Autonomous Underwater Vehicle and Ocean Modelling Networks: GOAT2 2000 Conference Proceedings, pp. 315-322.

9. Zwillinger Daniel. Standard Mathematical Tables and Formulae. 30th edition, CRC press, p 333.

Annex A – OPTIMAL OBSERVATION ANGLE BETWEEN TWO AUV LEGS

In the main text, we have shown that the mean angular probability of detection, $P_2(\phi)$, generated by two AUV legs achieves an optimum when the angle ϕ between the two legs is equal to $90\ \text{deg}$. We further show, in this Appendix, that this is in fact a global maximum. The proof is a generalization of the result shown in Fig. 12. It is true because of the shape and symmetry of the angular probability of detection with respect to $90\ \text{deg}$.

For the purpose of this Appendix, it is convenient to redefine aspect angle θ by shifting it to the left by $90\ \text{deg}$ such that the maximal angular probability of detection occurs at $0\ \text{deg}$, Fig. 24. There are many ways to prove that $P_2\left(\phi = \frac{\pi}{2}\right)$ is a global maximum. We choose to show that $P_2\left(\phi = \frac{\pi}{2}\right) > P_2\left(\phi = \frac{\pi}{2} + \varphi\right)$ for any φ. However, due to the periodicity of $f(\theta)$ it is sufficient to show that this is true for all φ ranging from $0\ \text{deg}$ to $90\ \text{deg}$.

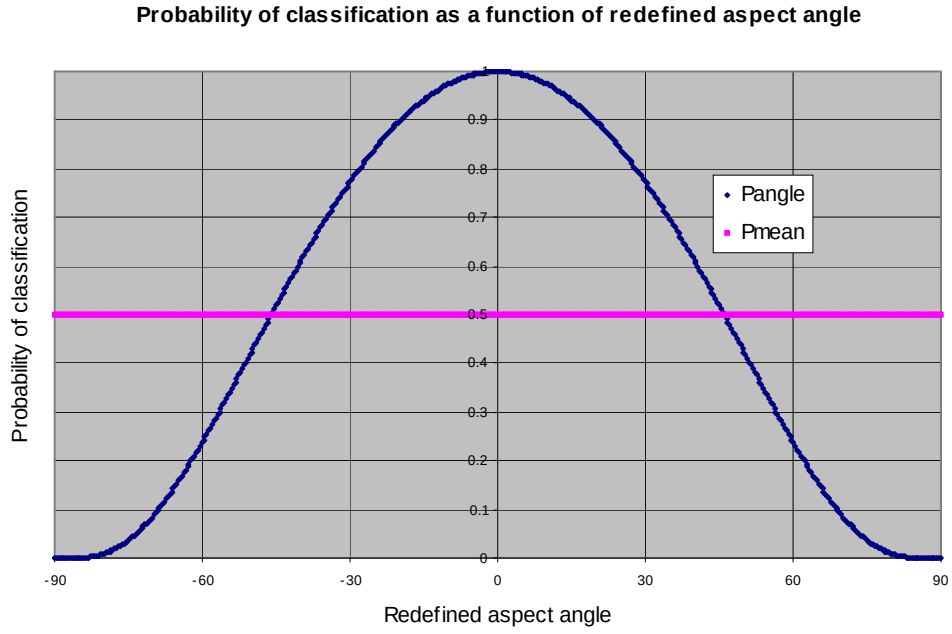

Figure 25. *Shifted mean angular probability of detection*

Recall that $P_2(\phi)$ is defined as:

$$P_2(\phi) = 1 - \frac{1}{\pi} \cdot \int_{-\frac{\pi}{2}}^{\frac{\pi}{2}} d\theta \cdot \left(1 - f(\theta)\right) \cdot \left(1 - f(\theta + \phi)\right) \tag{11}$$

Hence:

$$P_2\left(\frac{\pi}{2} + \varphi\right) = 1 - \frac{1}{\pi} \cdot \int_{-\frac{\pi}{2}}^{\frac{\pi}{2}} d\theta \cdot \left(1 - f(\theta)\right) \cdot \left(1 - f\left(\theta + \frac{\pi}{2} + \varphi\right)\right) \tag{12}$$

Since $f(\theta)$ is a periodic function with a period equals to 180 deg :

$$\begin{aligned} P_2\left(\frac{\pi}{2} + \varphi\right) &= 1 - \frac{1}{\pi} \cdot \int_{-\frac{\pi}{2}}^{\frac{\pi}{2}} d\theta \cdot \left(1 - f(\theta) - f\left(\theta + \frac{\pi}{2} + \varphi\right) + f(\theta) \cdot f\left(\theta + \frac{\pi}{2} + \varphi\right)\right) \\ &= \frac{2 \cdot \lambda_\theta}{\pi} - \frac{1}{\pi} \cdot \int_{-\frac{\pi}{2}}^{\frac{\pi}{2}} d\theta \cdot f(\theta) \cdot f\left(\theta + \frac{\pi}{2} + \varphi\right) \end{aligned} \tag{13}$$

where λ_θ is the scale compounded to the Johnson's curve defined in the main text. Thus, to show that $P_2\left(\phi = \frac{\pi}{2}\right)$ is a maximum is equivalent to show that $\int_{-\frac{\pi}{2}}^{\frac{\pi}{2}} d\theta \cdot f(\theta) \cdot f\left(\theta + \frac{\pi}{2}\right)$ is a minimum, in the sense that:

$$\int_{-\frac{\pi}{2}}^{\frac{\pi}{2}} d\theta \cdot f(\theta) \cdot f\left(\theta + \frac{\pi}{2} + \varphi\right) \geq \int_{-\frac{\pi}{2}}^{\frac{\pi}{2}} d\theta \cdot f(\theta) \cdot f\left(\theta + \frac{\pi}{2}\right) \tag{14}$$

Rewrite the left hand side as follows:

$$\begin{aligned} \int_{-\frac{\pi}{2}}^{\frac{\pi}{2}} d\theta \cdot f(\theta) \cdot f\left(\theta + \frac{\pi}{2} + \varphi\right) &= \int_{-\frac{\pi}{2}}^{0} d\theta \cdot f(\theta) \cdot f\left(\theta + \frac{\pi}{2} + \varphi\right) + \int_{0}^{\frac{\pi}{2}} d\theta \cdot f(\theta) \cdot f\left(\theta + \frac{\pi}{2} + \varphi\right) \\ &= \int_{0}^{\frac{\pi}{2}} d\theta \cdot \left[f(\theta) \cdot f\left(\theta - \frac{\pi}{2} - \varphi\right) + f(\theta) \cdot f\left(\theta + \frac{\pi}{2} + \varphi\right)\right] \end{aligned} \tag{15}$$

Similarly rewrite the right hand side as follows:

$$\int_{-\frac{\pi}{2}}^{\frac{\pi}{2}} d\theta \cdot f(\theta) \cdot f\left(\theta+\frac{\pi}{2}\right) = \int_{-\frac{\pi}{2}}^{0} d\theta \cdot f(\theta) \cdot f\left(\theta+\frac{\pi}{2}\right) + \int_{0}^{\frac{\pi}{2}} d\theta \cdot f(\theta) \cdot f\left(\theta+\frac{\pi}{2}\right)$$
$$= \int_{0}^{\frac{\pi}{2}} d\theta \cdot \left[f(\theta) \cdot f\left(\theta+\frac{\pi}{2}\right) + f(\theta) \cdot f\left(\theta-\frac{\pi}{2}\right) \right] \quad (16)$$

Subtract the right hand side to the left hand side:

$$A+B+C =$$
$$\int_{0}^{\frac{\pi}{2}} d\theta \cdot f(\theta) \cdot \left(f\left(\theta-\frac{\pi}{2}-\varphi\right) - f\left(\theta-\frac{\pi}{2}\right) \right) + \int_{0}^{\frac{\pi}{2}} d\theta \cdot f(\theta) \cdot \left(f\left(\theta+\frac{\pi}{2}+\varphi\right) - f\left(\theta+\frac{\pi}{2}\right) \right) \quad (17)$$

where

$$A = \int_{\varphi}^{\frac{\pi}{2}} d\theta \cdot f(\theta) \cdot \left(f\left(\theta-\frac{\pi}{2}-\varphi\right) - f\left(\theta-\frac{\pi}{2}\right) \right) + \int_{0}^{\frac{\pi}{2}-\varphi} d\theta \cdot f(\theta) \cdot \left(f\left(\theta+\frac{\pi}{2}+\varphi\right) - f\left(\theta+\frac{\pi}{2}\right) \right) \quad (18)$$

$$B = \int_{0}^{\varphi} d\theta \cdot f(\theta) \cdot \left(f\left(\theta-\frac{\pi}{2}-\varphi\right) - f\left(\theta-\frac{\pi}{2}\right) \right) \quad (19)$$

$$C = \int_{\frac{\pi}{2}-\varphi}^{\frac{\pi}{2}} d\theta \cdot f(\theta) \cdot \left(f\left(\theta+\frac{\pi}{2}+\varphi\right) - f\left(\theta+\frac{\pi}{2}\right) \right) \quad (20)$$

To prove $P_2\left(\phi=\frac{\pi}{2}\right)$ is a global maximum, we will show that $A, B, C \geq 0$. To help clarify the proof, we display Johnson's curves as a function of θ in Fig. 25. For illustration, we set $\varphi = 22.5\deg\left(\frac{\pi}{8}\right)$ and $\alpha_2 = 0.75$ while all other parameters remain unchanged. Note that we can remove the parameter λ_θ in the proof, as it is only a constant multiplied to Johnson's density distributions.

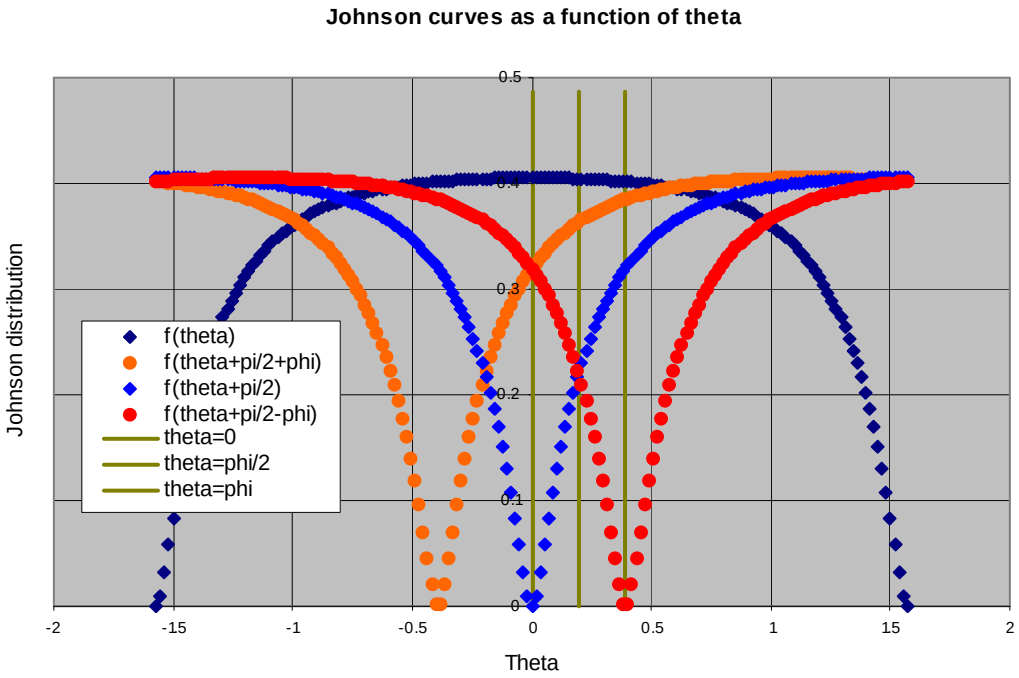

Figure 26. *Johnson curves*

$A \geq 0$

Make a change of variable in the second integral $\theta' = \theta + \varphi$ and knowing that $f(\theta)$ is a periodic function with period equals to 180 deg :

$$A = \int_{\varphi}^{\frac{\pi}{2}} d\theta \cdot f(\theta) \cdot \left(f\left(\theta - \frac{\pi}{2} - \varphi\right) - f\left(\theta - \frac{\pi}{2}\right) \right) + \int_{0}^{\frac{\pi}{2}-\varphi} d\theta \cdot f(\theta) \cdot \left(f\left(\theta + \frac{\pi}{2} + \varphi\right) - f\left(\theta + \frac{\pi}{2}\right) \right)$$

$$= \int_{\varphi}^{\frac{\pi}{2}} d\theta \cdot f(\theta) \cdot \left(f\left(\theta - \frac{\pi}{2} - \varphi\right) - f\left(\theta - \frac{\pi}{2}\right) \right) + \int_{\varphi}^{\frac{\pi}{2}} d\theta \cdot f(\theta - \varphi) \cdot \left(f\left(\theta + \frac{\pi}{2}\right) - f\left(\theta + \frac{\pi}{2} - \varphi\right) \right)$$

$$= \int_{\varphi}^{\frac{\pi}{2}} d\theta \cdot f(\theta) \cdot \left(f\left(\theta + \frac{\pi}{2} - \varphi\right) - f\left(\theta + \frac{\pi}{2}\right) \right) + \int_{\varphi}^{\frac{\pi}{2}} d\theta \cdot f(\theta - \varphi) \cdot \left(f\left(\theta + \frac{\pi}{2}\right) - f\left(\theta + \frac{\pi}{2} - \varphi\right) \right)$$

Rewrite the integrand as a product:

$$A = \int_{\varphi}^{\frac{\pi}{2}} d\theta \cdot \left(f(\theta - \varphi) - f(\theta) \right) \cdot \left(f\left(\theta + \frac{\pi}{2}\right) - f\left(\theta + \frac{\pi}{2} - \varphi\right) \right) \tag{21}$$

Since $f(\theta)$ is monotonous for θ between *zero* deg$(=0)$ and 90 deg$\left(\frac{\pi}{2}\right)$ then the first term of the integrand is non-negative i.e. $f(\theta-\varphi)-f(\theta)\geq 0$. Similarly, the second term of the integrand is also non-negative i.e. $f\left(\theta+\frac{\pi}{2}\right)-f\left(\theta+\frac{\pi}{2}-\varphi\right)\geq 0$. This is seen in Fig. 25. The light blue curve $\left(f\left(\theta+\frac{\pi}{2}\right)\right)$ is higher than the red curve $\left(f\left(\theta+\frac{\pi}{2}-\varphi\right)\right)$ for $\theta\in[\varphi,\pi]$ i.e. to the right of the third vertical line. Hence the integrand of A is non-negative and thus A itself is non-negative.

$B\geq 0$

Rewrite B as a sum of two integrals:

$$B=\int_0^{\frac{\varphi}{2}} d\theta\cdot f(\theta)\cdot\left(f\left(\theta-\frac{\pi}{2}-\varphi\right)-f\left(\theta-\frac{\pi}{2}\right)\right)+\int_{\frac{\varphi}{2}}^{\varphi} d\theta\cdot f(\theta)\cdot\left(f\left(\theta-\frac{\pi}{2}-\varphi\right)-f\left(\theta-\frac{\pi}{2}\right)\right)$$

Make a change of variable in the second integral $\theta'=\varphi-\theta$:

$$B=\int_0^{\frac{\varphi}{2}} d\theta\cdot f(\theta)\cdot\left(f\left(\theta-\frac{\pi}{2}-\varphi\right)-f\left(\theta-\frac{\pi}{2}\right)\right)+\int_0^{\frac{\varphi}{2}} d\theta\cdot f(\theta-\varphi)\cdot\left(f\left(\theta-\frac{\pi}{2}\right)-f\left(\theta-\frac{\pi}{2}-\varphi\right)\right)$$

where we have used the even parity of $f(\theta)$ and its period of 180 deg in the second integral. Rewrite the sum of two integrands as a product:

$$B=\int_0^{\frac{\varphi}{2}} d\theta\cdot\left(f(\theta)-f(\theta-\varphi)\right)\cdot\left(f\left(\theta-\frac{\pi}{2}-\varphi\right)-f\left(\theta-\frac{\pi}{2}\right)\right) \qquad (22)$$

For $\theta\in\left[0,\frac{\varphi}{2}\right]$, the first term of the integrand is non-negative i.e. $f(\theta)-f(\theta-\varphi)\geq 0$.

Similarly, the second term of the integrand is non-negative i.e. $f\left(\theta-\frac{\pi}{2}-\varphi\right)-f\left(\theta-\frac{\pi}{2}\right)\geq 0$.

This is shown in Fig. 25. The red curve $\left(f\left(\theta-\frac{\pi}{2}-\varphi\right)\right)$ is higher than the light blue curve $\left(f\left(\theta-\frac{\pi}{2}\right)\right)$ for $\theta\in\left[0,\frac{\varphi}{2}\right]$ i.e. between the first two vertical lines. Hence the integrand of B is non-negative and thus B itself is non-negative.

The proof for $C\geq 0$ is identical to that of B. So we have shown that $A, B, C\geq 0$. Hence, $A+B+C\geq 0$. This confirms that $P_2\left(\phi=\frac{\pi}{2}\right)$ is a global maximum. Note that we can show in a similar way that $P_2(\phi=0)$ is a global minimum.

List of symbols/abbreviations/acronyms/initialisms

AUV	Autonomous Underwater Vehicle
DND	Department of National Defence
K	(Koopman) Random search pattern
M	(Regular) Lawn Mowing pattern
MCM	Mine Counter Measure
MOE	Measure of Effectiveness
MOP	Measure of Performance
MU	Uneven Lawn Mowing pattern
ROV	Remotely Operated Vehicle
VB	Visual Basic computer language
Z	Zigzag search pattern

Distribution list

Document Number: DRDC CORA TM 2008-042

DRDC Atlantic/David Hopkin/John Fawcett

DRDC Atlantic/ Jim L Kennedy

DRDC Atlantic/ Jim S. Kennedy

DRDC Atlantic/Zahir Daya/Boris Vasiliev

DRDC Atlantic/Mae Seto/Vincent Myers/Francine Desharnais

DRDC Atlantic/Marcel Lefrancois

MARLANT/Paul Saunders/Michel Couillard/Peter Smith/Neil Carson

MARPAC/Ron Funk

DRDC CORA/Chief Scientist/Dale Reding

DRDC CORA/MORT/Alex Bourque

DRDC CORA/JSORT/Van Fong

DRDC CORA/CORT/Paul Massel/Ed Emonds

NORAD/Jean Denis Caron/Sean Bourdon/Cherie Gott

NURC/E. Bovio/Ron Kessel

NC3A/Sylvie Martel

DRDC CORA Library (HC + PDF)

DRDKIM (PDF)

This page intentionally left blank.

DOCUMENT CONTROL DATA

(Security classification of title, body of abstract and indexing annotation must be entered when the overall document is classified)

1. ORIGINATOR (the name and address of the organization preparing the document. Organizations for whom the document was prepared, e.g. Centre sponsoring a contractor's report, or tasking agency, are entered in section 8.)

DRDC CORA
101 Colonel By Drive, Pearkes Building, Ottawa, Ontario
K1A 0K2

2. SECURITY CLASSIFICATION (overall security classification of the document including special warning terms if applicable).

UNCLASSIFIED

3. TITLE (the complete document title as indicated on the title page. Its classification should be indicated by the appropriate abbreviation (S,C,R or U) in parentheses after the title).

Autonomous Underwater Vehicles Conducting Mine Counter Measure Exploratory Operations

4. AUTHORS (Last name, first name, middle initial. If military, show rank, e.g. Doe, Maj. John E.)

Nguyen Bao U, Hopkin Dave, Yip Handson

5. DATE OF PUBLICATION (month and year of publication of document)

October 2008

6a. NO .OF PAGES (total containing information Include Annexes, Appendices, etc).

53

6b. NO. OF REFS (total cited in document)

9

7. DESCRIPTIVE NOTES (the category of the document, e.g. technical report, technical note or memorandum. If appropriate, enter the type of report, e.g. interim, progress, summary, annual or final. Give the inclusive dates when a specific reporting period is covered).

Technical Memorandum

8. SPONSORING ACTIVITY (the name of the department project office or laboratory sponsoring the research and development. Include address).

Defence R&D Canada - Atlantic
PO Box 1012
Dartmouth, NS, Canada B2Y 3Z7

9a. PROJECT OR GRANT NO. (if appropriate, the applicable research and development project or grant number under which the document was written. Please specify whether project or grant).

9b. CONTRACT NO. (if appropriate, the applicable number under which the document was written).

10a ORIGINATOR'S DOCUMENT NUMBER (the official document number by which the document is identified by the originating activity. This number must be unique to this document.)

DRDC CORA TM 2008-042

10b OTHER DOCUMENT NOs. (Any other numbers which may be assigned this document either by the originator or by the sponsor.)

DRDC CORA

11. DOCUMENT AVAILABILITY (any limitations on further dissemination of the document, other than those imposed by security classification)

(x) Unlimited distribution
( ) Defence departments and defence contractors; further distribution only as approved
( ) Defence departments and Canadian defence contractors; further distribution only as approved
( ) Government departments and agencies; further distribution only as approved
( ) Defence departments; further distribution only as approved
( ) Other (please specify):

12. DOCUMENT ANNOUNCEMENT (any limitation to the bibliographic announcement of this document. This will normally correspond to the Document Availability (11). However, where further distribution (beyond the audience specified in (11) is possible, a wider announcement audience may be selected).

13. ABSTRACT (a brief and factual summary of the document. It may also appear elsewhere in the body of the document itself. It is highly desirable that the abstract of classified documents be unclassified. Each paragraph of the abstract shall begin with an indication of the security classification of the information in the paragraph (unless the document itself is unclassified) represented as (S), (C), (R), or (U). It is not necessary to include here abstracts in both official languages unless the text is bilingual).

Recent improvements in Autonomous Underwater Vehicle (AUV) technologies are making them increasingly attractive as mine hunting platforms by extending the reach of the sensors and weapons that are used in these operations. In this paper, we describe novel concepts of operations for AUVs performing Mine Counter Measure (MCM) exploratory operations. These concepts maximize the MCM effectiveness and minimize resources in MCM exploratory operations. In particular, the paper describes how previously un-modelled characteristics such as the aspect and range dependencies of mine detection show a significant influence on the mission effectiveness of a side scan sonar based system.

14. KEYWORDS, DESCRIPTORS or IDENTIFIERS (technically meaningful terms or short phrases that characterize a document and could be helpful in cataloguing the document. They should be selected so that no security classification is required. Identifiers, such as equipment model designation, trade name, military project code name, geographic location may also be included. If possible keywords should be selected from a published thesaurus. e.g. Thesaurus of Engineering and Scientific Terms (TEST) and that thesaurus-identified. If it not possible to select indexing terms which are Unclassified, the classification of each should be indicated as with the title).

Autonomous Underwater Vehicles
Sonar
Probability of detection
Range
Aspect angle
Multiple looks
Concept of operations
Search patterns
Optimization
Dorado
Mines
Mine Counter Measure exploratory operations
Random search
Measures of Effectiveness
Measures of Performance
Monte Carlo simulation

DRDC CORA

www.drdc-rddc.gc.ca